

# Detection of dynamic strain using an SOA-fiber ring laser and an arrayed waveguide grating demodulator\*

WANG Hao, TAO Chuanyi\*\*, GAO Xiaofeng, ZHU Yueqing, WU Yiran, and ZHANG Jing

Chongqing Key Laboratory of Green Energy Materials Technology and Systems, School of Science, Chongqing University of Technology, Chongqing 400054, China

(Received 18 October 2021; Revised 22 December 2021)

©Tianjin University of Technology 2022

In this letter, a fiber Bragg grating (FBG) dynamic strain sensing system using a semiconductor optical amplifier (SOA)-fiber ring laser (FRL) and an arrayed waveguide grating (AWG) demodulator is proposed. Due to the characteristics of SOA, it can act as the gain medium as well as light source. The AWG module is used as the wavelength demodulator. It is shown that SOA-based FRL sensors can accurately respond to  $1.5 \mu\text{e}$  dynamic strain signal with high frequency up to 120 kHz and almost no distortion in the waveforms. Experimental results show that the system can be used for acoustic testing, such as underwater ultrasonic detection and external impact monitoring. In addition, the simultaneous dual-channel demodulated system is investigated in detail to verify the multiplexing. This dynamic strain sensing system can be widely utilized in structural health monitoring because of its high stability, low cost and good multiplexability.

**Document code:** A **Article ID:** 1673-1905(2022)06-0331-7

**DOI** <https://doi.org/10.1007/s11801-022-1163-1>

Recent years, fiber Bragg grating (FBG) sensors are popular sensing elements and have a wide application of strain monitoring in the area of structural health monitoring, aerospace and medical cases due to the features of electromagnetic interference resistance, compact structure, and high sensitivity<sup>[1]</sup>. Moreover, FBG can also be utilized in temperature measurement and distributed strain. When the grating is disturbed by the external environment, the Bragg wavelength will change. We can get the environmental parameters of FBG by measuring its wavelength shift<sup>[2]</sup>. The key technology in terms of FBG sensing system is mainly determined by demodulating the wavelength shift<sup>[1,3]</sup>. In recent years, there are various of interrogation methods such as scanning methods using either a tunable laser or tunable filter and through interferometric methods<sup>[4,5]</sup>. The scanning methods are especially suitable for the detection of static or low frequency measurements<sup>[6]</sup>. As for high-frequency dynamic strain measurements, the interferometric methods are more likely to be chosen, but it has the poor signal-to-noise ratio (SNR)<sup>[5-7]</sup>.

The interrogation methods for monitoring dynamic strains are main techniques which seem to be primarily divided into two means. One is to directly measure the reflection (or transmission) spectrum of FBG, and the other is transforming wavelength shift into the change of output light intensity based on intensity modulation. The latter method is a very attractive approach to fabricate a

simple FBG vibration sensor<sup>[8]</sup>. The basic principle of edge filter is that it can directly transform the wavelength shift into intensity change. LIU et al<sup>[9]</sup> demonstrated a multiplexing method for FBGs-based ultrasonic sensors including a fiber-ring laser. Add-drop filters are used to achieve multiplexing, and the lasers corresponding to different channels from the common path are routed into different paths, each of which has a separate span of erbium-doped fiber (EDF), which makes a complicated multiplex and high cost. Recently, we proposed a multiplexed fiber ring laser (FRL) sensing system whose cavity consists of a non-tunable fiber Fabry-Perot filter (FFPF) and an FBG array for dynamic strain detection<sup>[10]</sup>. But the use of fiber bandpass filters to separate multiple lasing modes of the ring laser output usually decreases the number of multiplexing channels.

Based on some of the demodulated structures mentioned above, we further presented a simple intensity interrogation scheme based on an arrayed waveguide grating (AWG) module, which is an effective method with high speed, high capacity, and intelligent optical fiber communication. AWG module is a major technology and research hotspot in the field of optical fiber communication<sup>[11,12]</sup>. The AWG was first proposed by SMITH<sup>[13]</sup> in 1988 and was further developed in the following years by TAKAHASHI et al<sup>[14]</sup> who reported the first devices operating in the long wavelength window. In addition, due to mismatch of thermal expansion coefficient

\* This work has been supported by the National Natural Science Foundation of China (No.51874064), and the Project of Graduate Innovation in Chongqing University of Technology (No.gzlcx20223295).

\*\* E-mail: taochuanyi@cqut.edu.cn

of materials in AWG and optical fiber, AWG is very sensitive to temperature, which can easily result in optical wavelength drift<sup>[15]</sup>. A wide variety of interrogation configurations have already been proposed because of the characteristics of AWG module. JOHN et al<sup>[16]</sup> found that the noise dependence on the relative overlap of the AWG and FBG spectra was significant and the implement of a semiconductor optical amplifier (SOA) to boost light intensity at the detectors could significantly improve performance with an improvement in the *SNR* up to 200%. In this letter, we demonstrate the detection of dynamic strain based on an SOA-FRL coupled with an AWG interrogator. The SOA is a gain medium with a dominant inhomogeneous broadening property<sup>[17]</sup>. Owing to the characteristics of high *SNR* and stable output of the SOA-based FRL sensor<sup>[18]</sup>, there is a good response when FBG is subjected to dynamic micro-strains at high frequencies.

Fig.1 shows the experimental setup of the SOA-based FRL sensor system<sup>[19]</sup>. The ring laser cavity is composed of an SOA, an isolator, a 90:10 coupler, a circulator and an FBG (or FBG array). The Thorlabs' SOA1117S SOA (with a saturation output power of 9 dBm, a small signal gain of 20 dB, operating over a 34 nm bandwidth in the C-band) is chosen as the gain medium of the ring laser<sup>[20]</sup>. The SOA in ring cavity is selected as the gain medium as well as light source for improving the *SNR*. The amplified spontaneous emission (ASE) emitted from SOA is filtered using a wavelength selective filter consisting of an FBG and an optical circulator<sup>[21]</sup>. The 90% of light signal filtered out by FBG returns to the loop, the rest of which is coupled out. This process will continue until the equilibrium state is finally reached and the laser is emitted at the Bragg wavelength. The isolator in this configuration is utilized to prevent reverse transmission of light.

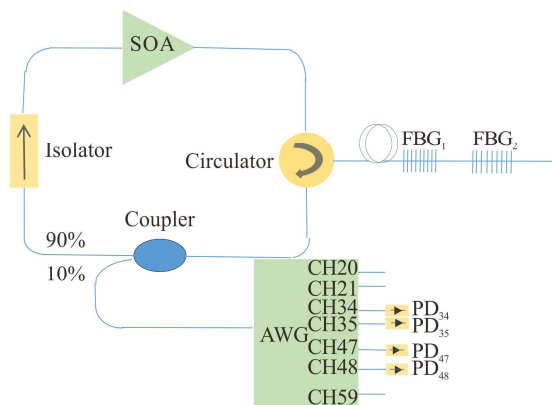


**Fig.1 Experimental setup of the SOA-based FRL sensor system with an AWG demodulator**

The static output spectra from SOA-based FRL sensor at different pumping currents ranging from 200 mA to 350 mA are shown in Fig.2(a). An AQ6370D optical spectrum analyzer is employed at the output port of this cavity. As shown in Fig.2(a), there is a similar feature

between the laser output and the FBG reflective spectrum. The typical time-dependent oscillation output power under 350 mA pumping current shown in Fig.2(b) indicates the lasing mode is stable. As an example of a single strain sensor, the central wavelength of FBG is selected as 1 550.05 nm. The output power has increased from -5 dBm to -0.15 dBm when there is no strain signal. This is related to the theory that higher bias currents result in a higher population inversion percentage, which in turn increases the stimulated emission and generates a higher output power<sup>[22]</sup>. In this experiment, the pump current of 350 mA is more suitable because the output does not increase significantly when the current exceeds 350 mA.

The AWG module is chosen as the wavelength demodulator. The AWG we selected contains 40 channels with 100 GHz channel spacing. The central wavelength range covers from 1 530.329 nm to 1 561.394 nm. As an example of a single strain sensor, the central wavelength of FBG in this experiment is selected as 1 550.05 nm, so the channels of AWG are chosen as CH34 and CH35.

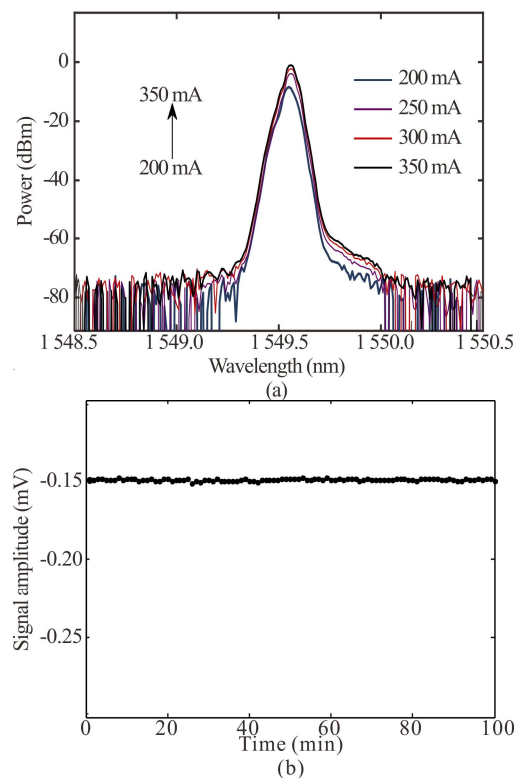


**Fig.2 (a) Output spectra based on an SOA-based FRL sensor under different pumping currents; (b) Stable output of an SOA-based FRL**

The typical principle of AWG wavelength demodulation is shown in Fig.3. The FBG reflective spectrum is right in between two adjacent channels of the AWG module. Strain induces the wavelength shift of the sensing FBG reflection spectrum, consequently, the overlap between the reflection spectrum of the sensing FBG and the two adjacent transmission spectra of the AWG will change accordingly. Generally, when there is a slight

fluctuation in FBG central wavelength, it will induce that one light output increases and the other decreases for two adjacent AWG channels. Therefore, the wavelength shift of the sensing FBG is successfully converted into intensity change of two adjacent channels.

With a Gaussian-shaped profile, the output spectrum of FRL can be set up as

$$I(\lambda) = I_0 \exp \left[ -4 \ln 2 \left( \frac{\lambda - \lambda_B}{\Delta\lambda} \right)^2 \right], \quad (1)$$

where  $I_0$  under Bragg wavelength  $\lambda_B$  is the output intensity of the laser.  $\Delta\lambda$  represents an output laser 3 dB of bandwidth. We define  $P_n$  as the output light power of the adjacent channels of the AWG. It can be determined by the following equation<sup>[22]</sup>

$$P_n = (1-L) \int_0^\infty I(\lambda) T_{AWG,n}(\lambda) d\lambda, \quad (2)$$

where  $T_{AWG,n}$  represents the transmission spectrum of AWG channel  $n$ ,  $L$  represents the total attenuation factor of the whole measurement system, and  $\lambda$  represents the wavelength. The power ratio of  $S$  is defined as follows

$$S = \frac{P_{n+1} - P_n}{P_{n+1} + P_n}, \quad (3)$$

where  $S$  stands for the difference-to-sum ratio in light intensity between two adjacent AWG channels, which can indicate the change in intensity to some extent when the FBG is subjected to dynamic strain. The center wavelength of each FBG has a value corresponding to  $S$ . From Eq.(3), it can be seen that when FBG is subjected to dynamic strain, the change of the center wavelength of the sensing FBG can be converted into the change of output intensity of the overlap between two adjacent channels of the AWG and the center wavelength of the FBG<sup>[23]</sup>.

Fig.4 shows the reflection spectrum of the sensing FBG ( $\lambda=1\ 550.05\ \text{nm}$ ) and transmission spectra of two adjacent AWG channels ( $\lambda_{CH34}=1\ 550.116\ \text{nm}$ ,  $\lambda_{CH35}=1\ 549.315\ \text{nm}$ ). The 3-dB bandwidth of FBG we used is 0.20 nm. It can be seen from Fig.4 that the center wavelength of a sensing FBG is in between two AWG channels.

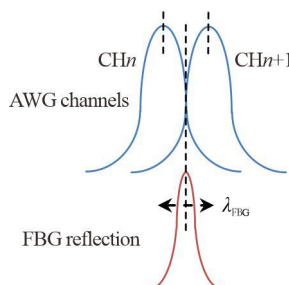


**Fig.3 Schematics of the reflection spectrum of the sensing FBG and the transmission spectra of adjacent AWG channels**

In the detection experiment of dynamic strain, the optical adhesives are used to glue the FBG sensor and the piezoelectric transducer (PZT) together. The PZT actuator is driven by sinusoidal electric signals generated from a

function generator. A dynamic strain with the frequency range from 48 kHz to 120 kHz and the same amplitude of 1.5  $\mu\text{e}$  is applied to the FBG sensor, which is centered at 1 550.05 nm with a 0.2 nm bandwidth. Fig.5(a) shows the oscilloscope traces for detection of dynamic strain signals under different driving frequencies, which is without electronic filtering. As can be seen from Fig.5(b), the SNRs range from 4.7 dB to 7.7 dB with the demodulated frequencies from 48 kHz to 120 kHz. This means that as the frequency changes, the SNR remains stable and there is no significant attenuation. The frequency spectrum of the dynamic strain signals is shown in Fig.5(c). This system has good response to high frequency dynamic micro-strain. The frequency of the detected dynamic signal is exactly consistent with the driving frequency of the PZT.

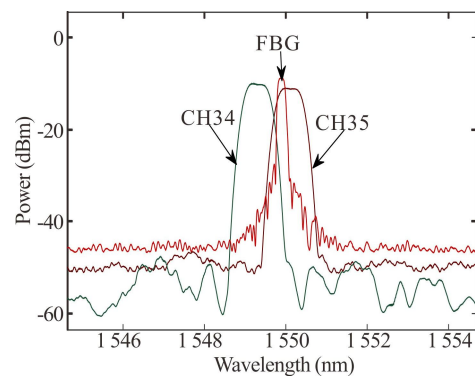


**Fig.4 Reflection spectrum of the sensing FBG and transmission spectra of two adjacent AWG channels (CH34 and CH35)**

After detecting the dynamic strain signal, the application of the sensing system in ultrasonic testing is presented. Different vibration devices may have different effects on measuring frequency range of AWG demodulated system. An ultrasonic cleaner with frequency of 33 kHz as a vibration device is used and the device is shown in Fig.6. The FBG with central wavelength of 1 550.05 nm is immersed under water at the temperature of 25 °C. The contact between the vibrating grating and the inner wall of ultrasonic cleaning machine is avoided to prevent interference. Therefore, the FBG is hung so that its axis is perpendicular to the water surface and in the middle of the ultrasonic cleaning machine.

When the underwater ultrasonic signal is applied to the FBG sensor, the demodulated signal of the sensor system is converted into an electrical signal by a pair of photodetectors and then displayed on the oscilloscope. Fig.7 shows the results of demodulation of the underwater ultrasonic signal by the semiconductor ring laser dynamic strain sensing system based on AWG demodulation. Fig.7(a) is the transient response signal when the ultrasonic cleaner starts to work. The oscillation starts with small amplitude and then the amplitude gradually increases to a stable value. It can be seen from Fig.7(b) that the underwater ultrasonic signal periodically oscillates and there is no significant change in frequency. Fig.7(c) shows a continuous underwater ultrasonic signal when the ultrasonic

cleaner is working stably. Therefore, the semiconductor ring laser dynamic strain sensing system based on AWG demodulation can play an important role in the ultrasonic detection of structural health monitoring.

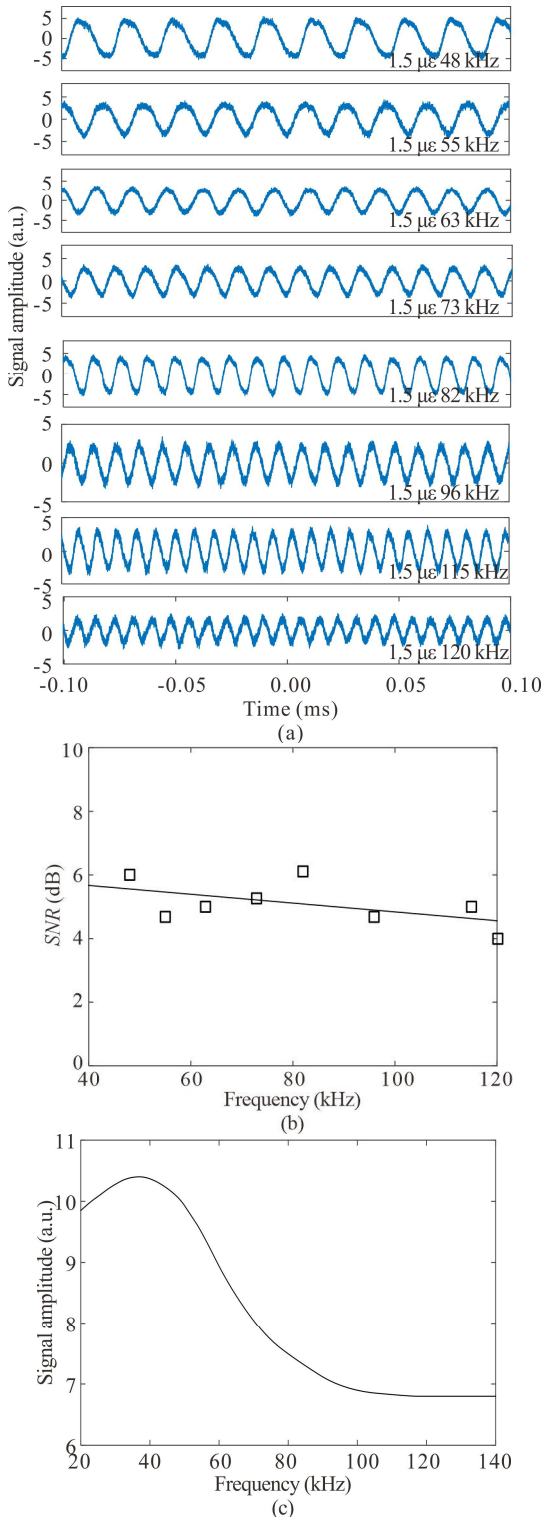


**Fig.5 (a) Demodulated results of the FBG sensor system by applying a dynamic strain with an amplitude of  $1.5 \mu\epsilon$  and a frequency of 48—120 kHz; (b) Relationship between the SNR and the demodulated frequency; (c) Frequency spectrum of the dynamic strain signals**

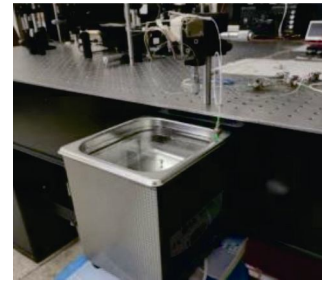


**Fig.6 Setup for ultrasonic detection under water**

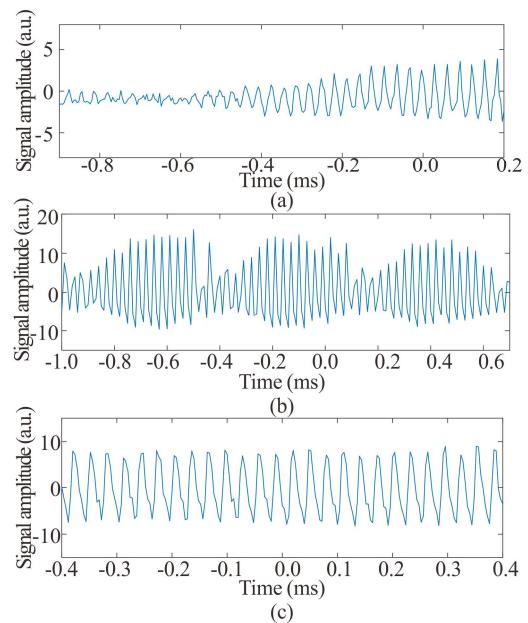


**Fig.7 Demodulated results of ultrasonic signals under water: (a) 33 kHz transient signal; (b) Ultrasonic oscillation signal; (c) Continuous ultrasonic signal**

The detection experiment of impact is carried out in order to demonstrate the response of the dynamic strain sensing system to the impact load of objects. As shown in Fig.8, a ball bearing with diameter about 3 mm is used to hit the aluminum plate. The point of impact is 20 cm away from the axial extension line of the FBG sensor on the surface of the aluminum plate. The oscilloscope is applied to capture the demodulated signal, and the trigger level is set slightly higher than the noise level. Fig.9 shows the time response signal and time-frequency signal of the impact acoustic emission signal respectively. It can be seen from the initial time response signals presented in Fig.9(a) and (c) that the frequencies of the PZT sensor and the FBG sensor are about 46 kHz and 60 kHz, respectively. The acoustic emission sensing signal oscillation starts from a small amplitude and the frequency gradually decreases. Therefore, the semiconductor ring laser dynamic strain sensing system based on the demodulation of AWG is expected to be applied to the monitoring of acoustic emission caused by the impact of objects.

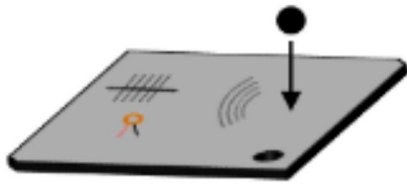


**Fig.8 Schematic of detection of acoustic emission signal induced by foreign impact**

Furthermore, dual-channel multiplexing using the SOA-FRL system with two FBG sensors has been demonstrated. Two FBG sensors with Bragg wavelengths of 1 539.54 nm and 1 550.05 nm are cascaded in one fiber. The signal output from the corresponding two pairs of AWG adjacent channels (CH47/CH48 and CH34/CH35) is monitored simultaneously. We applied a sinusoidal dynamic strain with a frequency of 5 kHz and an amplitude of  $2 \mu\epsilon$  on the sensor FBG<sub>1</sub> ( $\lambda_B=1\ 539.54\ \text{nm}$ ) and that with a frequency of 11 kHz and an amplitude of  $2 \mu\epsilon$  on the sensor FBG<sub>2</sub> ( $\lambda_B=1\ 550.05\ \text{nm}$ ). Fig.10 shows the multiplexing demodulated results of FRL sensors. Multiple lasing modes in this FRL configuration are feasible. The two dynamic strain signals are demodulated separately, and there is no obvious crosstalk between them. This demonstrates that a multichannel SOA-FRL dynamic strain sensor coupled with an AWG spectral demodulator can be used for multiplexed demodulation of several FBG dynamic strains sensors.

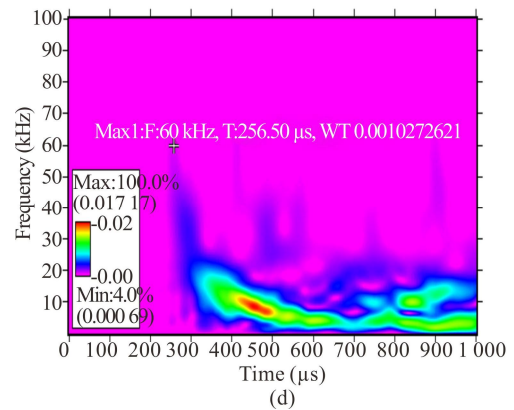
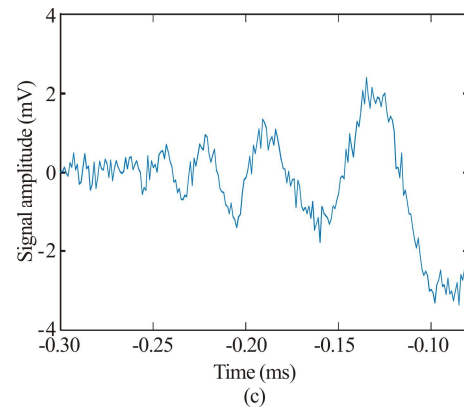
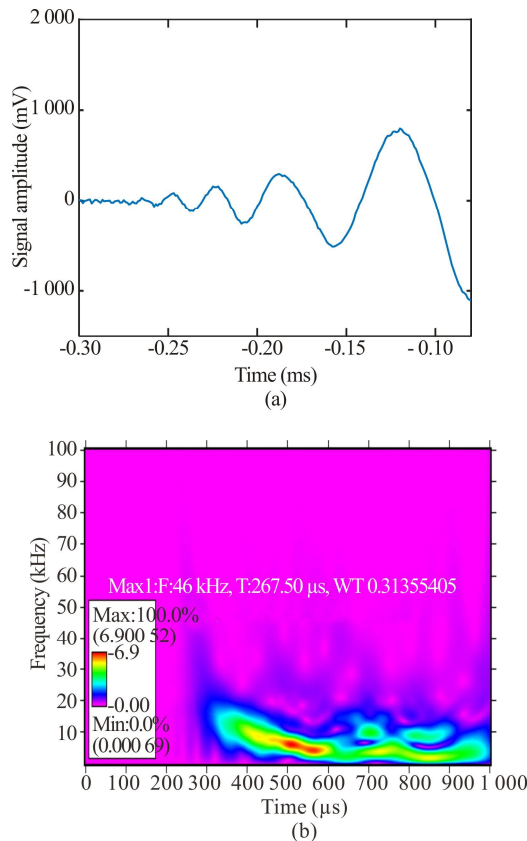


**Fig.9 Demodulation results of acoustic emission signals from the impact: (a) Time response signal from PZT; (b) Time-frequency signal from PZT; (c) Time response signal from FBG; (d) Time-frequency signal from FBG**

Generally, dynamic strain sensing system is one of the effective methods for detecting cracks in composite structures and predicting potential failures. However, current dynamic strain sensing systems based on electronic PZTs have many limitations. Traditional electronic dynamic strain transducers have many disadvantages, such as bulky, not easily embedded in composites, susceptible to electromagnetic interference and so on<sup>[24,25]</sup>. Compared with electronic dynamic strain transducers, FBG sensors are the most promising optical sensing elements because of the characteristics of small size, light weight, and can detect dynamic strains without being affected by electromagnetic interference<sup>[26]</sup>. The performance comparison between the fiber optic sensor and conventional piezo-based sensor (740B02, PCB PIEZOTRONICS) is shown in Tab.1.

The above experimental results presented preliminary work towards the development of a compact FBG sensor interrogator system based on multi-channel SOA sensor coupled with AWG demodulator technology for applications where size and weight are critical for operation. The test results of the SOA-FRL-AWG sensor system demonstrated the demodulated principle of the AWG demodulator for the accurate measurement of the spectral shift of the FBG sensors when the sensors are exposed to high-frequency stress-strain, vibration, and acoustics<sup>[9]</sup>. The sensor system is easy to produce at low cost because

it uses commercially available telecommunication components. The sensing channel of the sensor system can reach up to 20 because the AWG we selected contains 40 channels. The 100 GHz channel spacing of AWG produces a dynamic range of 1 600 pm, corresponding to a strain range of  $\sim 1\ 300\ \mu\epsilon$ . The static strain range can be improved by increasing the AWG channel spectral width. An increase in the AWG spectral width will reduce the measurand resolution because the associated FBG wavelength shift will result in a lower change in intensity<sup>[16]</sup>. Although a detection of the strain at  $1.5\ \mu\epsilon$  and 120 kHz is demonstrated in the experiment, higher frequencies can still be detected. The sensitivity of the sensing system is limited by the optical thermal noise, so the actual sensitivity is better than  $1.5\ \mu\epsilon/\text{Hz}$ . Compared with the current SOA-FRL-AWG sensor system, the FRL-FFPF sensor system reported previously can only realize the multiplexing of up to 8 FBG sensors due to the limitation of band-pass filter<sup>[10]</sup>.

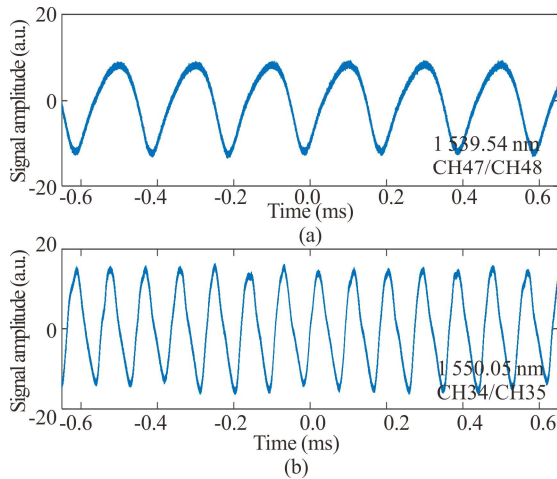


**Fig.10** Multiplexing demodulated results of FRL sensor system, in which two FBG sensors are excited by (a) a 5 kHz,  $2\ \mu\epsilon$  dynamic strain and (b) an 11 kHz,  $2\ \mu\epsilon$  dynamic strain, respectively

**Tab.1** Comparison of dynamic strain sensitivity between typical piezo-based sensor and fiber optical sensor

Parameter	Piezo-based sensor	Fiber optic sensor
Multiplexability and sensor channels	Not readily multiplexable; single channel	Multiplexable; up to 20 channels
Frequency range	0.5—100 000 Hz	1—120 000 Hz
Broadband resolution	0.6 nε	0.1 με
Dimensions	Bulky	Small size and light weight
Compatibility	Not easily embedded in composites	Compatible with composite materials
EMI	Susceptible to EMI	Immune to EMI
Cost	Inexpensive	Expensive
Temperature	Intolerant of high temperature (-53 °C—121 °C)	High temperature resistance (>600 °C)
Transmission stability	Poor signal transmission stability	Stable transmission in optical fiber

Currently, photonic integrated circuits (PICs) have gradually developed into a mature technology, connecting various optical devices or optoelectronic devices through optical path, such as a semiconductor laser, electro-optic modulator, photodetector, optical amplifier, optical multiplexer/demultiplexer, etc<sup>[27,28]</sup>. However, it is not easy to integrate the SOA FRL source in PICs. The present sensing system is expected to achieve miniaturization through photonic integration by using a reflective semiconductor optical amplifier (RSOA) source<sup>[6]</sup>. A desired PIC design of the RSOA-FBG fiber cavity laser sensing system may include an RSOA source, a 10:90 optical coupler, the FBG sensors and the photodetector array. The RSOA source and FBG sensors form an adaptive fiber cavity laser. The spectral drift of the FBG sensor due to dynamic strains causes the wavelength shifts of the laser output accordingly, which is subsequently demodulated by an AWG. It is believed that the AWG demodulated system based on the PIC will be the future development direction.

In conclusion, in this work, we present an SOA-FRL sensing system to interrogate the dynamic strain signals with an AWG device. The system has a good demodulated response for high-frequency dynamic micro-strain signals up to 120 kHz. The sensing channel of the sensor system can reach up to 20 for the selected AWG. The 100 GHz channel spacing of AWG produces a dynamic range of 1 600 pm, corresponding to a strain range of  $\sim 1\ 300\ \mu\epsilon$ . A dual-channel FBG sensing system based on the SOA-FRL and the AWG wavelength demodulator is discussed, which shows the potential for wavelength multiplexing of FBG sensors. The sensor system is easy to produce at low cost because it uses commercially available telecommunication components. This configuration is expected to be miniaturized and get better applicability through photonic integration.

**Statements and Declarations**

The authors declare that there are no conflicts of interest related to this article.

**References**

- [1] WANG C, YAO J. Ultrafast and ultrahigh-resolution interrogation of a fiber Bragg grating sensor based on interferometric temporal spectroscopy[J]. *Lightwave technology*, 2011, 29(19): 2927-2933.
- [2] JULIO P R, JOSE G S, DRAGOS P, et al. Fast interrogation of fiber Bragg gratings with electro-optical dual optical frequency combs[J]. *Sensors*, 2016, 16(12): 2007.
- [3] LEE H D, KIM G H, EOM T J, et al. Linearized wavelength interrogation system of fiber Bragg grating strain sensor based on wavelength-swept active mode locking fiber laser[J]. *Lightwave technology*, 2015, 33(12): 2617-2622.
- [4] FOMITCHOV P A, PAVEL. Response of a fiber Bragg grating ultrasonic sensor[J]. *Optical engineering*, 2003,

- 42(4): 956-963.
- [5] JIANG X H, TAO C Y, XIAO J J, et al. Fiber-ring laser strain sensing system with two-wave mixing interferometric demodulation[J]. *Acta optica sinica*, 2021, 41(13): 1306021. (in Chinese)
- [6] WEI H M, KRISHNASWAMY S. Comparative assessment of erbium fiber ring lasers and reflective SOA linear lasers for fiber Bragg grating dynamic strain sensing[J]. *Applied optics*, 2017, 56(13): 3867-3874.
- [7] QIAO Y, ZHOU Y, KRISHNASWAMY S. Adaptive demodulation of dynamic signals from fiber Bragg gratings using two-wave mixing technology[J]. *Applied optics*, 2006, 45(21): 5132-5142.
- [8] INAMOTO K, TANAKA S, YOKOSUKA H, et al. SOA-based multi-wavelength fiber laser for FBG vibration sensor array[C]//*Optical Fiber Sensors 2006*, October 23-27, 2006, Cancun, Mexico. Washington, DC: OSA, 2006: 83.
- [9] LIU T, HU L L, HAN M. Multiplexed fiber-ring laser sensors for ultrasonic detection[J]. *Optics express*, 2013, 21(25): 30474-30480.
- [10] MAOL M, TAOC Y, ZHANG J, et al. Multiplexed dynamic strain sensing system based on a fiber ring laser using a non-tunable fiber Fabry-Perot filter[J]. *Applied optics*, 2020, 59(8): 2375-2379.
- [11] ZHENG Y, DUAN J A. Transmission characteristics of planar optical waveguide devices on coupling interface[J]. *Optik*, 2013, 124(21): 5274-5279.
- [12] ZHENG Y, DUAN J A. Alignment algorithms for planar optical waveguides[J]. *Optical engineering*, 2012, 51(10): 2002-2009.
- [13] WANG W, TAO C Y, WANG H, et al. Sagnac fiber interferometer with the population grating for fiber Bragg grating dynamic strain sensing[J]. *Optoelectronics letters*, 2021, 17(12): 723-728.
- [14] TAKAHASHI H, SUZUKI S, KATO K, et al. Arrayed-waveguide grating for wavelength division multi/demultiplexer with nanometre resolution[J]. *Electronics letters*, 1990, 26(2): 87-88.
- [15] ZHENG Y, LI J P, GAO P P, et al. Packaging experiments of arrayed waveguide grating[J]. *Optik*, 2018, 168: 179-183.
- [16] JOHN R N, READ I, MACPHERSON W N. Design considerations for a fibre Bragg grating interrogation system utilizing an arrayed waveguide grating for dynamic strain measurement[J]. *Measurement science & technology*, 2013, 24(7): 075203.
- [17] YEH C H, CHI S. Fiber-fault monitoring technique for passive optical networks based on fiber Bragg gratings and semiconductor optical amplifier[J]. *Optics communications*, 2006, 257(2): 306-310.
- [18] KIM S, KWON J, KIM S, et al. Multiplexed strain sensor using fiber grating-tuned fiber laser with a semiconductor optical amplifier[J]. *IEEE photonics technology letters*, 2001, 13(4): 350-351.
- [19] ZHANG J, TAO C Y, XIAO J J, et al. Dynamic strain sensing system using a SOA based fiber ring laser with fiber Bragg gratings and an AWG demodulator[C]//*Health Monitoring of Structural and Biological Systems XV*, March 22-27, 2021, Online Only, California, United States. Bellingham: SPIE, 2021.
- [20] CHEN R, TAO C Y, JIANG X H, et al. Detection of dynamic signals from multiplexed SOA-based fiber-ring laser sensors[J]. *Applied optics*, 2018, 57(35): 10159-10163.
- [21] AHMAD H, OOI H C, SULAIMAN A H, et al. SOA based fiber ring laser with fiber Bragg grating[J]. *Microwave and optical technology letters*, 2008, 50(12): 3101-3103.
- [22] DUTTA N K, WANG Q. Semiconductor optical amplifiers[J]. *Encyclopedia of modern optics*, 2013, 18(24): 308-316.
- [23] SU H, HUANG X G. A novel fiber Bragg grating interrogating sensor system based on AWG demultiplexing[J]. *Optics communications*, 2007, 275(1): 196-200.
- [24] TRESSLER J F, ALKOY S, NEWNHAM R E. Piezoelectric sensors and sensor materials[J]. *Journal of electroceramics*, 1998, 2(4): 257-272.
- [25] HU N, FUKUNAGA H, MATSUMOTO S, et al. An efficient approach for identifying impact force using embedded piezoelectric sensors[J]. *International journal of impact engineering*, 2007, 34(7): 1258-1271.
- [26] KIRIKERA G R, BALOGUN O, KRISHNASWAMY S. Adaptive fiber Bragg grating sensor network for structural health monitoring: applications to impact monitoring[J]. *Structural health monitoring*, 2010, 9(1): 5-16.
- [27] PUSTAKHOD D, KLEIJN E, WILLIAMS K, et al. High-resolution AWG-based fiber Bragg grating Interrogator[J]. *IEEE photonics technology letters*, 2016, 28(20): 2203-2206.
- [28] LI H Q, GAO W T, LI E, et al. Investigation of ultra small  $1 \times N$  AWG for SOI-based AWG demodulation integration microsystem[J]. *IEEE photonics journal*, 2015, 7(6): 1-7.